AIAA 4th APPLIED AERODYNAMICS CONFERENCE

A COLLECTION OF TECHNICAL PAPERS
SAN DIEGO, CALIFORNIA
JUNE 9-11, 1986

Free-Vortex Method Simulation of Unsteady Airfoil/Vortex Interaction

Tatsuo Fujinami*
Department of Aerospace Engineering and Engineering Mechanics
University of Texas at Austin, Austin, Texas 78712

George S. Dulikravich**
Department of Aerospace Engineering
Pennsylvania State University, University Park, PA 16802

Ahmed A. Hassan+
Department of Mechanical and Aerospace Engineering
Arizona State University, Tempe, Arizona

ABSTRACT

An accurate computer program using free-vortex method is developed to simulate compressible unsteady interactions between vortex wakes and isolated airfoils and between oscillating tandem airfoils. Second-order vortex panel method with a compressibility correction was used to compute disturbed flowfields over airfoils. Several flow patterns due to interactions between vortex wakes and airfoils were simulated.

NOMENCLATURE

A = Influence coefficient matrix
a = Local speed of sound
C_p = Pressure coefficent
f = Nonlinear term in full potential equation
$G(t)$ = Unsteady Bernoulli constant
M = Number of free vortices
N = Number of node points used to discretize airfoils
$\vec{n}$ = Unit vector normal to an airfoil surface
P = Static pressure
$\vec{r}$ = Position vector
$\vec{U}_\infty$ = Free stream velocity vector
$\vec{U}$ = Translation velocity of the origin of moving coordinates
$\vec{V}$ = Absolute velocity vector
α = Angle of attack
Γ = Circulation
γ = Strength of a vortex
δ = Dirac delta function
ξ,η = Coordinates associated with airfoil elements
ρ = Local fluid density
ϕ = Velocity potential function
χ = Fundamental solution of Laplace's equation
$\vec{\Omega}$ = Angular velocity of a moving coordinates
$\int ds$ = Line integral
$\int dA$ = Surface integral

Subscripts

B = Airfoil surface
c = Convection term
∞ = At infinity

Superscripts

$-$ = Wake
$*$ = Non-dimensional quantity

INTRODUCTION

A reliable numerical method capable of computing strong interaction between vortex wakes and isolated or multi-component airfoils is important for aerodynamic and aeroelastic analysis and design. In order to analyze unsteady flowfields, for example leading edge separations from delta wings, interactions between helicopter blades and their wakes during forward flight, and vortices shedding from oscillating multi-component airfoils, a methodology to describe separate wakes and disturbed flowfields must be established. Because of the complexity of the unsteady flow phenomena, efficient simulation using Navier-Stokes equations with turbulence modeling are not presently available for engineering applications.

Free-vortex methods have been currently investigated by numerous authors [1,2,3] and used to simulate separate wake motions and disturbed flowfields. The basic advantages of free-vortex methods over finite volume or finite element methods are computational efficiency and the applicability to large scale simulation of flows over arbitrarily shaped configurations. Free point-vortices are commonly used to track separated wakes from sharp corners or smooth surfaces. The strength of each free vortex is determined using unsteady Kutta-Zhukowski condition and Kelvin's theorem. Separated wakes are constructed from free vortices shed from separation points at each discrete time step.

Surface panel methods, widely used for steady aerodynamic analysis and design, can be also used to compute unsteady potential flowfields over airfoils. It is well known that the accuracy of panel methods depends on the choice of surface singularities [4] and the treatment of Kutta-Zhukowski condition [5]. The present method is an extension of surface panel methods to unsteady flow simulation including wake interactions with airfoils. Second-order vortex panel method with a conventional compressibility correction was chosen to compute steady and unsteady compressible flows over airfoils. Using linear finite element expansion for unknown surface vortex strengths, exact Kutta condition can be explicitly enforced. Several example calculations including interactions between free vortices and airfoils will be described.

* Manager, Recruit Co.,Ltd. RCS Division
Student member AIAA

** Associate Professor
Member AIAA

+ Assistant Professor
Member AIAA

ANALYSIS

Assuming a quasi-steady, inviscid, and irrotational flow over the entire domain, conservation of mass can be written as

$$\nabla^2\phi = f \tag{1}$$

where f is a non-linear term representing compressibility effect. Using a moving coordinate system [6,7], this term becomes

$$f = (1/a^2)\ [\vec{V}_c\cdot\nabla(\vec{V}_c\cdot\nabla\phi) + \frac{1}{2}\nabla\phi\cdot\nabla\ (\nabla\phi\cdot\nabla\phi) + 2\nabla\phi\cdot\nabla\ (\vec{V}_c\cdot\nabla\phi)] \tag{2}$$

where V_c is the convection velocity given as

$$\vec{V}_c = -\vec{U} - \vec{\Omega}\times\vec{r} \tag{3}$$

The local speed of sound, a, becomes

$$a^2 = a_\infty^2 - (\gamma - 1)\ [\vec{V}_c\cdot\nabla\phi + \frac{1}{2}\nabla\phi\cdot\nabla\phi] \tag{4}$$

For incompressible fluids, the mass conservation equation reduces to

$$\nabla^2\phi = 0 \tag{5}$$

The velocity potential is quasi time-dependent. The solution of the continuity equation is determined by the time-dependent boundary condition on the airfoil surface, that is, the location of the airfoil changes as time proceeds and eq.(1) or (5) is solved at each discretized time step. The unsteady pressure distribution for incompressible fluid flow can be obtained using the unsteady Bernoulli equation as

$$\frac{\partial\phi}{\partial t} - \vec{V}\cdot(\vec{U} + \vec{\Omega}\times\vec{r}) + \frac{V^2}{2} + \frac{P_\infty}{\rho} = G(t) \tag{6}$$

Choosing $G(t) = P_\infty / \rho$, the unsteady pressure coefficient can be written as

$$C_P = \frac{P - P_\infty}{\frac{1}{2}\rho U_\infty^2} = 1 - 2\frac{\partial\phi}{\partial t} + 2\vec{V}\cdot(\vec{U} - \vec{\Omega}\times\vec{r}) - \frac{V^2}{2} \tag{7}$$

Vortex Panel Formulation

The discretization of eq.(1) can be performed using Greer's formula with the fundamental solution χ which satisfies eq.(8).

$$\nabla^2\chi = \delta(x - \xi,\ y - \eta) \tag{8}$$

Then the potential in the flowfield can be evaluated as

$$\phi = \int_{\partial\Omega}(\chi\frac{\partial\phi}{\partial n} - \phi\frac{\partial\chi}{\partial n})ds + \int_\Omega f\chi\, dA \tag{9}$$

For incompressible fluids this reduces to

$$\phi = \int_{\partial\Omega}(\chi\frac{\partial\phi}{\partial n} - \phi\frac{\partial\chi}{\partial n})ds \tag{10}$$

This is the basic equation of Morino's doublet panel formulation [8]. It is easily modified into vortex panel formulation used by Mook [6,9]. The resulting vortex panel equation becomes [9]

$$\int_B \gamma\frac{\partial\theta}{\partial n}\,ds = \vec{U}_\infty\cdot\vec{n}_i \tag{11}$$

where $\theta = \arctan\left((y - \eta)/(x - \xi)\right)$

Vortex panel method is prefered over a combined source-vortex panel method [9] since only vortex strengths have to be determined. This is particularly important for unsteady flow simulations, because the determination of unknown vortex strengths must be repeated at each time step.

Unsteady Kutta-Zhukowski Condition

For inviscid fluid flow, the fluid must leave smoothly at the trailing edge. This Kutta condition can be interpreted as a zero pressure jump across the trailing edge [2,6,10]. Using eq.(7) for unsteady pressure coefficient, the pressure coefficient jump ΔC_P across the trailing edge becomes

$$\Delta C_P = C_{P_L} - C_{P_U} = -2\frac{\partial}{\partial t}(\Delta\phi) - 2\vec{V}_c\cdot\nabla(\Delta\phi) = 0 \tag{12}$$

where $\Delta\phi$ is the potential jump between the upper and lower sides of the trailing edge given by $\Delta\phi = \phi_U - \phi_L$.
The convection velocity V_c of the wake at the trailing edge is obtained as

$$\vec{V}_c = \frac{1}{2}\nabla(\phi_U + \phi_L) - \vec{U} - \vec{\Omega}\times\vec{r}$$

Rewriting eq.(12), we get

$$\Delta C_P = -2\frac{D\Gamma}{Dt} = 0 \tag{13}$$

where substantial derivative is $\frac{D}{Dt} = \frac{\partial}{\partial t} + \vec{V}_c\cdot\nabla$ and the potential jump $\Delta\phi$ is equivalent to the instantaneous circulation Γ around the airfoil. Employing the forward differencing in time, eq.(13) can be discretized as

$$\frac{\Gamma^{n+1} - \Gamma^n}{\Delta t} + (\vec{V}_c^{\,n}\cdot\nabla)\Gamma^n = 0 \tag{14}$$

Rearranging eq.(14), we get the circulation change $\Delta\Gamma$ due to the unsteady motion of the airfoil as

$$\Delta\Gamma^n = \Gamma^{n+1} - \Gamma^n = -\Delta t\{A_x\,(V_{x_U} - V_{x_L}) + A_y\,(V_{y_U} - V_{y_L})\} \tag{15}$$

where
$$A_x = \frac{1}{2}(V_{x_U} + V_{x_L}) + V_{U_x} + V_{\Omega_x}$$
$$A_y = \frac{1}{2}(V_{y_U} + V_{y_L}) + V_{U_y} + V_{\Omega_y}$$

Also V_{U_x}, V_{U_y}, V_{Ω_x}, and V_{Ω_y} are the velocity components of the fluid on the upper and lower sides of the trailing edge, respectively.

V_{U_x}, V_{U_y}, V_{Ω_x}, and V_{Ω_y} represent the velocity components due to the solid body motion of the airfoil. Eq.(15) explicitly provices the circulation of each free-vortex shed from the trailing edge. If the flow is steady, eq.(13) reduces to

$$\vec{V}_c\cdot\nabla(\Delta\phi) = 0 \tag{16}$$

For symmetric three-dimensional problems, eq.(16) simplifies to [10]

$$\omega_x V_{c_z} - \omega_z V_{c_x} = 0 \qquad (17)$$

For two-dimensional problems, because $V_{c_x} \neq 0$ at the trailing edge, eq.(17) becomes

$$\omega_z = 0 \qquad (18)$$

Eq.(18) is a form of the steady state Kutta-Zhukowski condition asserted by conventional thin airfoil theory, that is, the bound vortex strength at the trailing edge must vanish in order to satisfy the Kutta condition.

Free Vortex Method

The wake separated from the trailing edge or the airfoil surface is simulated using free point-vortices. The velocity potential of a free point-vortex is

$$\bar{\phi} = -\frac{\bar{\gamma}}{2\pi}\theta \qquad (19)$$

For unsteady flow analysis the free point-vortices are generated at separation points at each time step because of the time change of total circulation around the airfoil. The strengths of new free vortices are explicitly determined using eq.(15). The free vortices constituting unsteady wakes interact with each other and are convected downstream at their local instantaneous convection velocities. Because of the inviscid fluid assumption, the strengths of point-vortices remain constant and the sum of circulations of all bound and free vortices also remains constant according to Kelvin's theorem.

NUMERICAL PROCEDURE

In order to discretize vortex panel equation (eq.11), the linear finite element expansion for unknown vortex strengths was employed. Linear expansion is convenient for the explicit enforcement of exact Kutta-Zhukowski condition at the trailing edge. This means that

$$\gamma_1 = \gamma_N = 0 \qquad (20)$$

A parabolic curve fitting for surface panel geometry was used to obtain the second-order accuracy [11]. The resulting set of linear algebraic equations with Kutta-Zhukowski condition equation (eq.20) can be written as

$$\sum_{j=2}^{N-1} A_{ij}\,\gamma_j = B_i \qquad (21)$$

$$1 \le i \le N-1$$

When the interaction between two airfoils is considered, the set of linear equations becomes

$$\sum_{j=2}^{N-1} A_{ij}\,\gamma_j = B_i \qquad (22)$$

$$1 \le i \le N-1\ ,\quad i \neq NN\ ,\quad j \neq NN,\ NN+1$$

For unsteady flow problems, the moving boundary surface effect and the disturbed velocity effect due to the motion of the wake must be taken into account to solve the panel equation (eq.11). Then the set of linear equations can be written as

$$\sum_{j=2}^{N-1} A_{ij}\,\gamma_j = (+\vec{U} + \vec{\Omega}\times\vec{r})\cdot\vec{n}_i + \sum_{k=1}^{M} \bar{A}_{ik}\,\bar{\gamma}_k \qquad (23)$$

$$1 \le i \le N-1$$

For both steady and unsteady computations, the set of linear equations is solved using least-squares method since the system is over-determined. Once the system is solved, the new free point-vortex strength is determined using unsteady Kutta condition equation (eq.15). At each time step this procudure is repeated and the wakes composed of free point-vortices are convected downstream with their independent velocities. The disturbed surface pressure distribution over the airfoils can be obtained from unsteady Bernoulli equation (eq.7).

COMPUTATIONAL RESULTS

Steady Flow Calculations

Firstly, computational results for steady flows are discussed. Comparisons between vortex panel solutions using Prandtl-Glauert compressibility correction and full potential equation solutions using finite area method [12] are shown in Fig.1. Conventional Pradtl-Glauert compressibility correction can be written as

$$c_p' = \frac{c_p}{\sqrt{1-M_\infty^2}}$$

An analysis of NACA0012 airfoil at zero degree angle of attack was performed using sixty four second-order panels. At free stream Mach number of 0.25 the panel solution shows good agreement with the finite area solution. At Mach number 0.5 the panel solution slightly differs from the full potential solution. This test case implies that for low subsonic flow computation, the second-order vortex panel solution with Prandtl-Glauert compressibility correction can provide acceptably accurate results. For high subsonic flow computations, the field source term $\iint_A f\,xdA$ in eq.(9) was discretized [13] to obtain better results.

However, the field source discretization requires additional computational time for each time step because the surface integral whose kernel includes several high-order derivatives must be evaluated. Paticularly, this nonlinear source term representing compressibility effect becomes quite complicated when a moving coordinate system is used. Therefore, for unsteady flow analysis, the simple algebraic compressibility correction was employed. This approach is not directly applicable to high subsonic or transonic flows such as the unsteady force analysis for helicopter blades. However, this method still provides first-order solutions which can be used as the initial data for further analysis.

Unsteady Flow Calculations

Four example calculations were performed for unsteady flow situations. The comparisons between unsteady Euler equation solution using finite volume method [14] and the second-order panel method solution are shown in Fig.2. Cambered NLR7301 airfoil having 16% thickness [14] was tested at free stream Mach number 0.5 undergoing pitching oscillatory mode given as $\theta = 0.5\sin(0.53\,t^*)$. Computational results at non-dimensional time $t^* = t'/(c/U_\infty) = 1.0$ and $t^* = 2.9$ are shown in Fig.2. Unsteady airfoil surface C_p distributions agree well for both cases. The advantages of this quasi-steady approach are computational efficiency and applicability to any arbitrary geometry including multi-component airfoils having arbitrary oscillatory modes. Furthermore, the comparisons shown in Fig.2 demonstrate the level of accuracy of this unsteady flow analysis method.

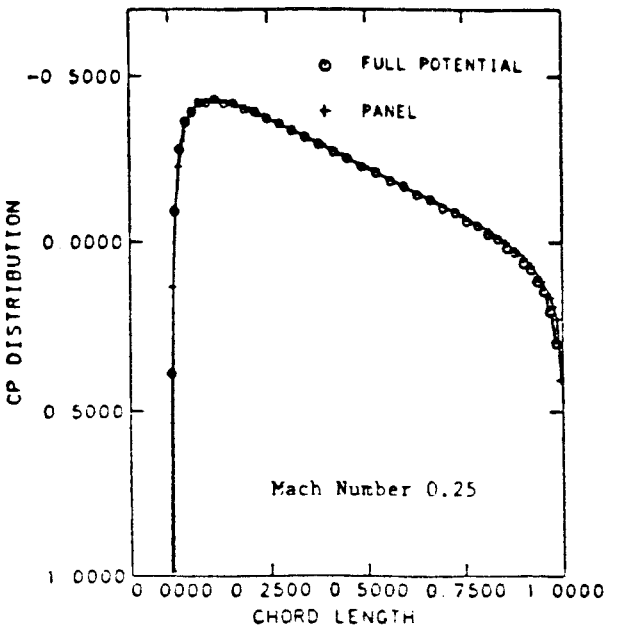

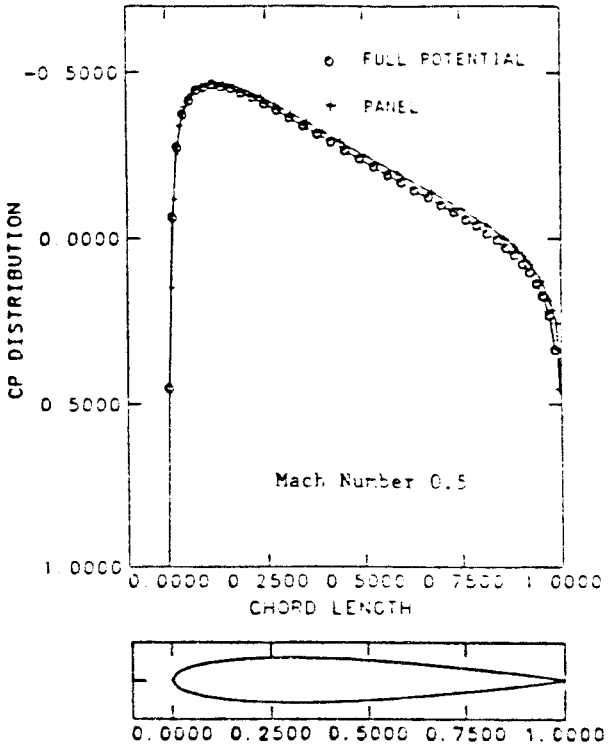

Figure 1. C_p Distribution Comparisons for Subsonic Flow

Interaction between a single free point-vortex and an isolated symmetric airfoil can be clearly observed in Fig.3. As a free point-vortex which is firstly located at 0.4 chord length upstream of the leading edge moves along x axis with constant velocity, the pressure coefficient C_p on the airfoil surface changes. Fig 3a shows the relative position between the free point-vortex and the airfoil and the corresponding surface C distribution at the first time step. Triangle and circle markers show upper and lower surface pressure coefficients C_p , respectively. No significant C_p change is observed. Fig.3b shows C_p distribution change due to interaction at the next time step. Because the vortex rotates in the clock

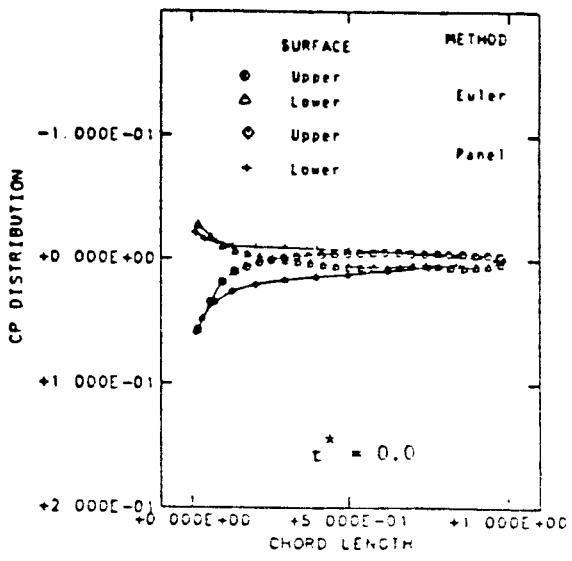

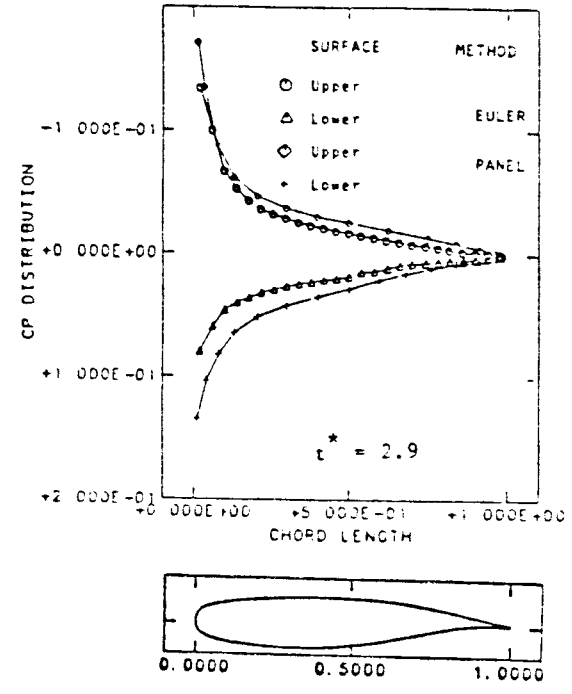

Figure 2. Unsteady C_p Distribution Comparisons

wise direction, the velocity vector induced by the free point-vortex on the upper airfoil surface is pointed against the free stream. Therefore, the upper surface C_p values around the airfoil leading edge are higher than ones on the lower side of the leading edge. The disturbance reaches its peak when the vortex is located in the mid-chord region as shown in Fig 3c and 3d. Finally, after the vortex passes over the airfoil, C_p distribution approaches the undisturbed value as shown in Fig 3e. Because the induced velocity is proportional to the inverse of the distance from the free point-vortex, the strong disturbance effect was observed only locally. Fig.4, 5, and 6 show time-dependent change of lift, drag, and moment coefficient, respectively. Strong interactions are seen only when the vortex is located close to the airfoil. When the free point-vortex passes above the airfoil, the strong negative lift is clearly observed in Fig.4. However, when the free point-

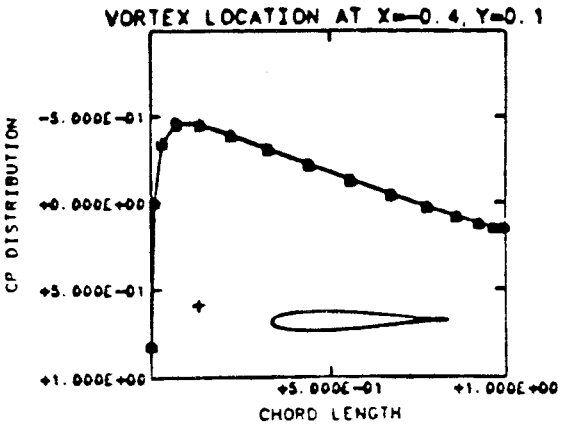

Figure 3a. A Free Point-Vortex Interaction with a Single Airfoil: Vortex Located at x/C = -0.4

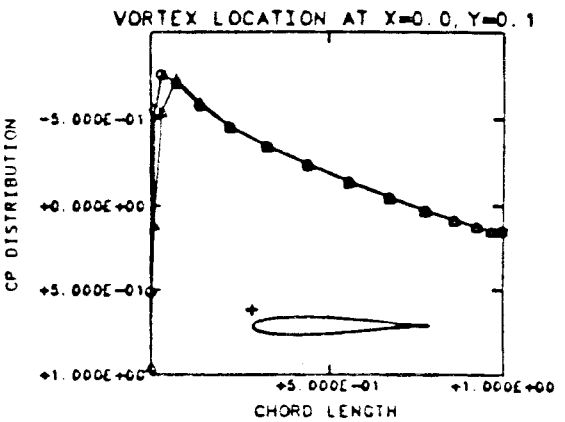

Figure 3b. A Free Point-Vortex Interaction with a Single Airfoil: Vortex Located at x/C = 0.0

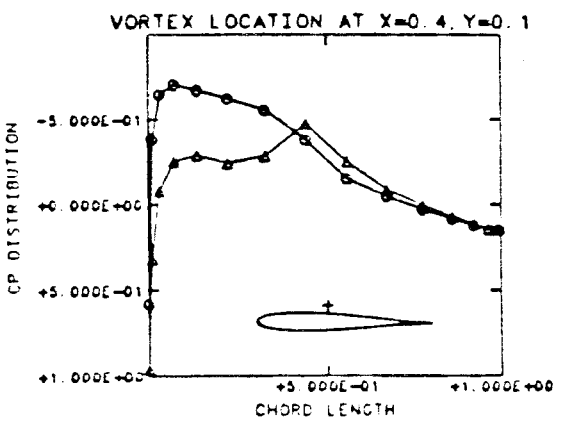

Figure 3c. A Free Point-Vortex Interaction with a Single Airfoil: Vortex Located at x/C = 0.4

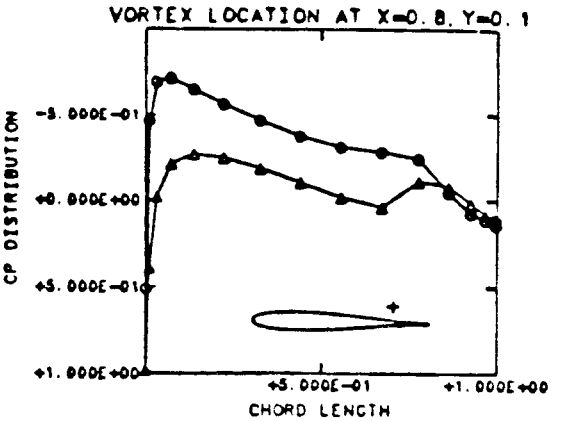

Figure 3d. A Free Point-Vortex Interaction with a Single Airfoil: Vortex Located at x/C = 0.8

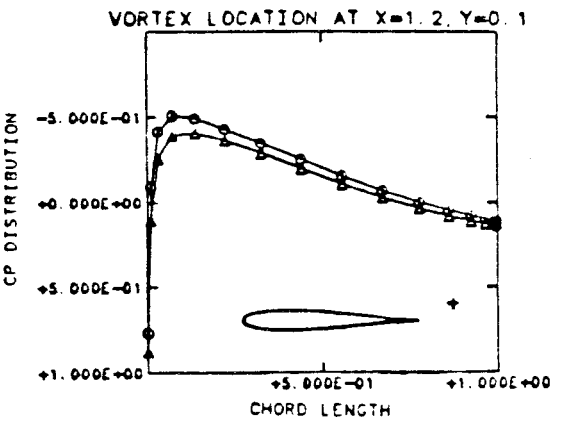

Figure 3e. A Free Point-Vortex Interaction with a Single Airfoil: Vortex Located at x/C = 1.2

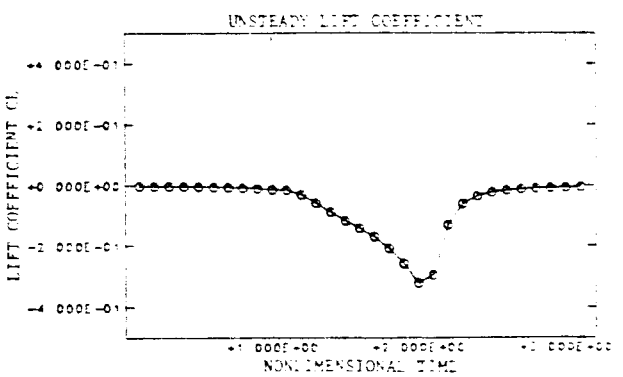

Figure 4. Unsteady Lift Coefficient for Airfoil/Vortex Interaction

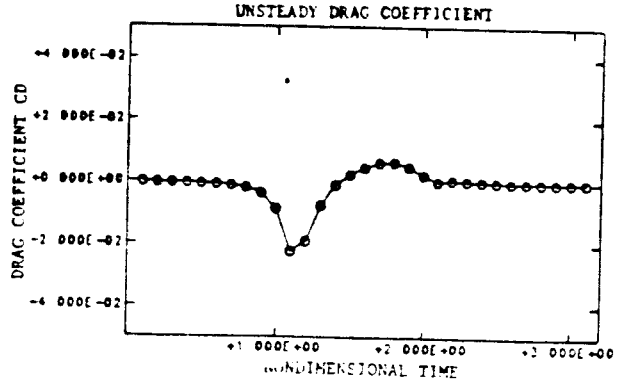

Figure 5. Unsteady Drag Coefficient for Airfoil/Vortex Interaction

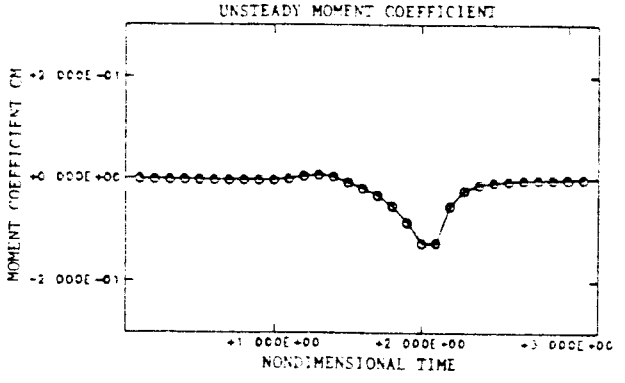

Figure 6. Unsteady Moment Coefficient for Airfoil/Vortex Interaction

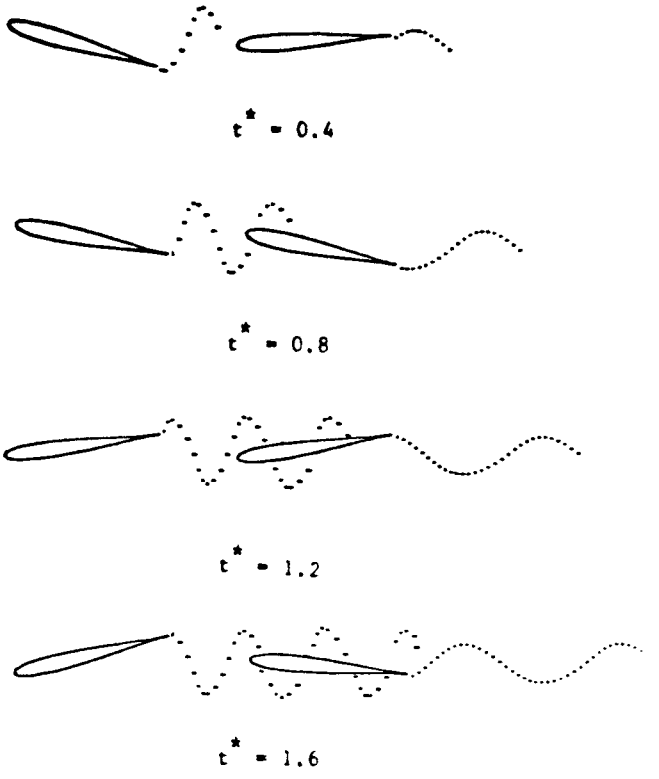

Figure 7. Wake Simulation for Double Airfoils

vortex is located about one chord length upstream of the airfoil, the lift coefficient asymptotically approaches the undisturbed value. The drag and moment coefficients exhibit the similar behavior.

Fig.7 shows sequence of flow patterns induced by the unsteady interactions between the vortex wakes of two oscillating airfoils. The first wake is intersected by the second airfoil at non-dimensional time $t^* = 0.8$ and the wake becomes divided into two parts. Then, each part of the wake propagates separately and locally creates its own disturbance over the second airfoil. Arbitrary motions of two airfoils including pitching and translating oscillatory modes with arbitrarily independent frequencies can be specified using this program [15]. Here, both airfoils are fluctuating with their own independent pitching frequencies. Pitching oscillatory mode can be specified as

$$\epsilon = A \sin(\Omega t^*)$$

For the first airfoil, $\Omega = 4\pi$ and $A = 5$ degrees were used and $\Omega = 2\pi$ and $A = 5$ degrees were chosen for the second airfoil. It should be noted that unsteady flow analysis using finite difference schemes is restricted only to low frequency and small magnitude oscillations. However, the integral equation approach as disscused in this paper can be applied to relatively high frequency and large magnitude oscillations as shown in this test case. Namely, the magnitude of the pitching velocity of the airfoil surface for this example is of the same order as the free stream velocity. It should be also noted that the quasi time dependent approach described here uses first-order accurate time discretization. Thus, the accuracy and the applicability of this free point-vortex method for calculations of high-frequency oscillations can be further improved. In addition, nonlinear effect due to compressibility becomes even more important than that in steady flow situations. Fig.8 shows C_p distributions at $t^* = 0.1$ and $t^* = 1.1$. At $t^* = 0.1$ the smooth C_p distribution is observed. On the other hand at $t^* = 1.1$ the local disturbance of the C_p distribution due to the presence of unsteady wake can be clearly depicted. Time-dependent changes of lift, drag, and moment coefficients are shown in Fig.9, 10, and 11. Smooth periodic changes of lift, drag, and moment begin to be disturbed after nondimensional time 0.8 at which the vortex wake shed from the first airfoil reaches the leading edge of the second airfoil.

Final example is the simulation of an oscillating airfoil with a flap. Three wake interactions from non-dimensional time $t^* = 0.2$ to $t^* = 0.8$ are shown in Fig.12. The airfoil is oscillating with pitching frequency $\Omega = 2\pi$ and magnitude $A = 5$ degrees. The flap is pitching around its own pivoting point as well as the main airfoil pivoting point, that is, the time-dependent surface coordinates of the second airfoil can be written as

$$Y = a_1 \sin(\Omega_1 t^*) + a_2 \sin(\Omega_2 t^*)$$

As time proceeds, two wakes from the main airfoil interact with the flap and part of the wakes propagates downstream around lower side of the flap. The remaining portion of the wakes is convected above the oscillating flap.

CONCLUSIONS

Computer program for calculating disturbed flowfields due to unsteady interaction among vortex wakes and moving airfoils was developed. Unsteady flow simulation for a number of different oscillatory modes over multi-component airfoils is possible using this code. The results show acceptable time accuracy and computational efficency. This work provides a basis for analysis of unsteady forces resulting from leading edge separations, interactions of helicopter blades and thier wakes during forward flight, and for inverse design of multi-component airfoils for minimized wake interactions. However, further improvements of compressibility corrections are necessary before applying this method to high subsonic flows.

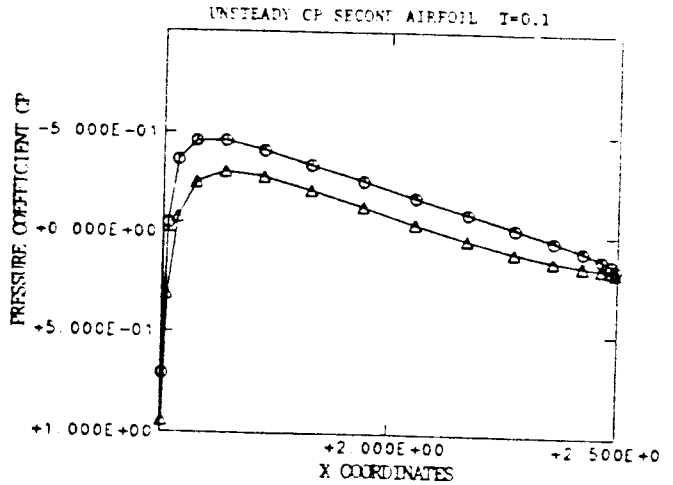

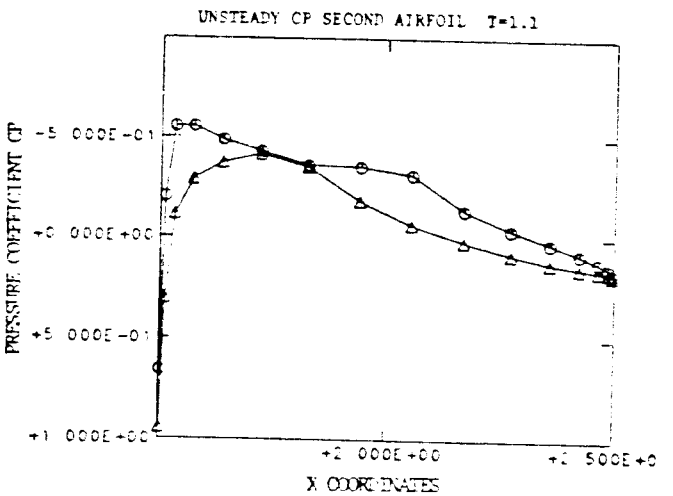

Figure 8. Unsteady C_p Distribution for Second Airfoil

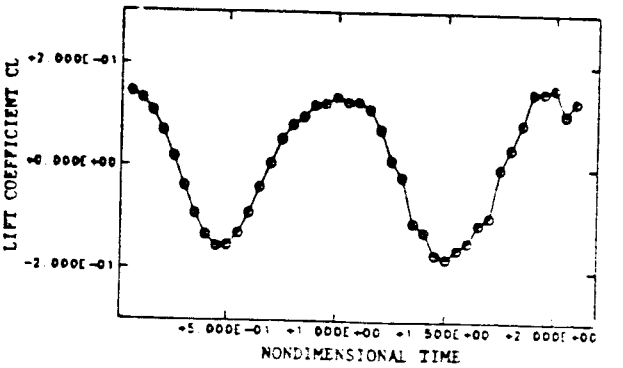

Figure 9. Unsteady Lift Coefficient for Second Airfoil

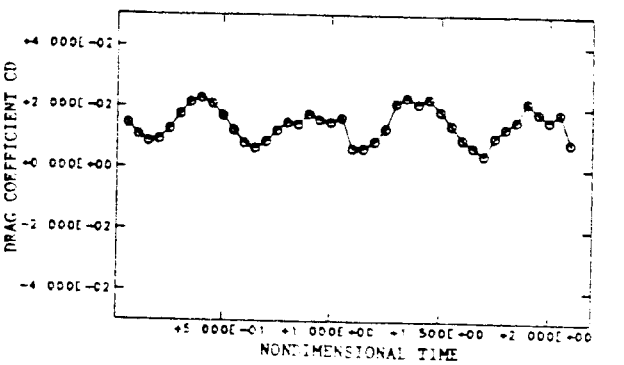

Figure 10. Unsteady Drag Coefficient for Second Airfoil

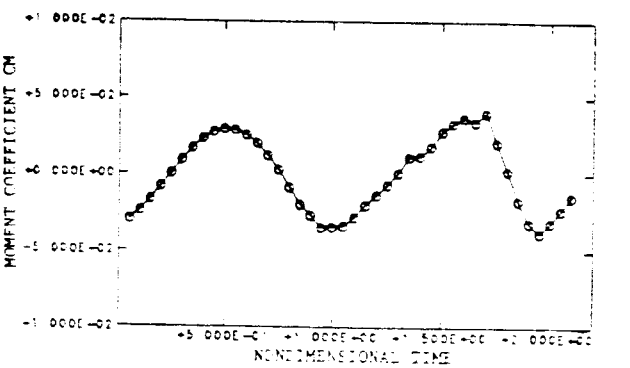

Figure 11. Unsteady Moment Coefficient for Second Airfoil

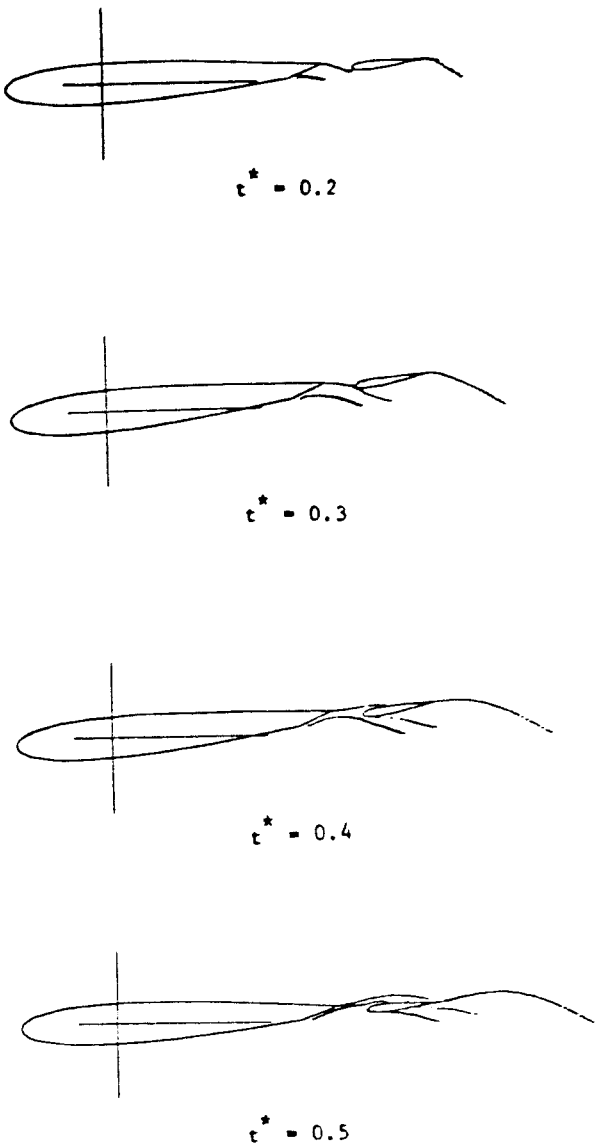

Figure 12. Wake Simulation for Airfoil and Flap

REFERENCES

1. Lewis,R.I,"Surface Vorticity Modelling of Separated Flows from Two-dimensional Bluff Bodies of Arbitrary Shape", J. Mechanical Engineering Science,Vol.23,No.1,pp.1-12,1981.
2. Katz,J.,"A Discrete Vortex Method for the Non-Steady Separated Flow Over an Airfoil", J. of Fluid Mechanics,Vol.12,pp.315-328,1981.
3. Leonard,A.,"A Review: Vortex Method for Flow Simulation", J. of Computationanl Physics, Vol.37,No.3, pp 289-335,1980.
4. Moran,J.,"An Introduction to Theoretical and Computational Aerodynamics", John Wiley and Sons, 1984.
5. Gostelow,J.P.,"Cascade Aerodynamics",Pergamon Press, 1984.
6. Mook,D.T. and Kim,M.J.,"Application of Continuous Vorticity Panels to General Unsteady Two-dimensional Lifting Flows",AIAA paper 85-0282, Reno, Nevada, 1985.
7. Caradonna,F.X. and Isom,M.P.,"Numerical Calculation of Unsteady Transonic Potential Flow Over Helicopter Rotor Blades",AIAA J. Vol.14, No.4, April, 1976, pp.482-488.
8. Morino,L.,"A General Theory of Unsteady Compressible Potential Aerodynamics", NASA CR-2464, 1974.
9. Fujinami,T."Computation of Unsteady Separated Compressible Flow Using Free-Vortex Method", M.Sc Thesis, Dept. of Aerspace Eng. and Eng. Mechanics, Univ. of Texas at Austin, August, 1985.
10. Kandil,O.A.,"A Nonlinear Hybrid Vortex Method for Wings at Large Angle of Attack", AIAA J. Vol.22, No.3, pp.329-336, 1984.
11. Hess,J.L.,"Higher-Order Numerical Solution of the Integral Equation for the Two-dimensional Neumar Problem", Computer Methods in Appl. Mechanics and Engineering, Vol.2, pp.1-15, 1973.
12. Dulikravich,G.S. and Olling,C.R.,"GSD28-FORTRAN Program for Analysis and Design of Shock-Free Transonic Airfoils and Turbomachinery Cascades Including Viscous/Inviscid Interaction", Computational Fluid Dynamics Group CFD Report 100-85, Dept. of Aerospace Eng. and Eng. Mechanics, Univ. of Texas at Austin, September, 1985.
13. Fujinami,T. and Dulikravich,G.S.,"Anaysis of Unsteady Compressible Cascade Flows Using Boundary Element and Free-Vortex Method", Sixth International Symposium on Finite Element Methods in Flow Problems, Antibes, France, June 16-20, 1986.
14. Magnus,R.J.,"Some Numerical Solutions of Inviscid, Unsteady Transonic Flows Over the NLR7301 Airfoil", NR061-214, January, 1978.